Supplementary Material to the manuscript:

A new laser device for ultra-rapid and sustainable aerosol sterilization

Supplementary Figures

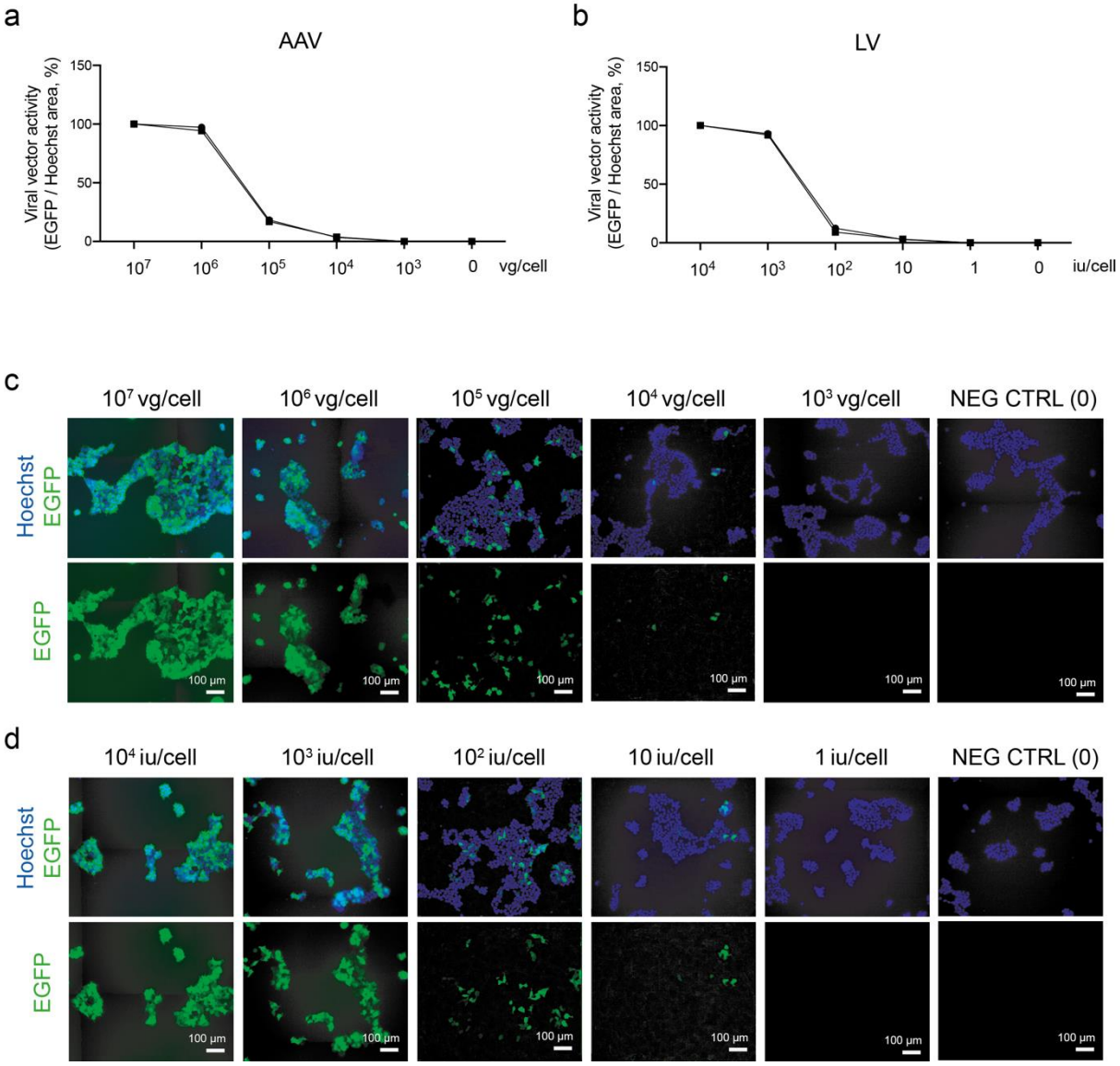

Supplementary Figure 1. Efficiency of AAV and LV transduction by serial dilutions. Stock solutions of AAV-EGFP (5 x 10^{12} vg/ml) and LV-EGFP (5 x 10^6 iu/ml) were serially diluted and added to HEK293 cells to determine the efficiency of transduction.

a. Quantification of AAV-EGFP vector activity, determined as a ratio between the $EGFP^+$ green area and the $Hoechst^+$ nuclear area, at the indicated dilutions.

b. Quantification of LV-EGFP vector activity, determined as a ratio between the $EGFP^+$ green area and the $Hoechst^+$ nuclear area, at the indicated dilutions.

c. Representative images of HEK293 cells expressing EGFP upon AAV transduction at the indicated doses. Negative control (NEG CTRL) corresponds to cells not exposed to the vector.

d. Representative images of HEK293 cells expressing EGFP upon LV transduction at the indicated doses. Negative control (NEG CTRL) corresponds to cells not exposed to the vector.

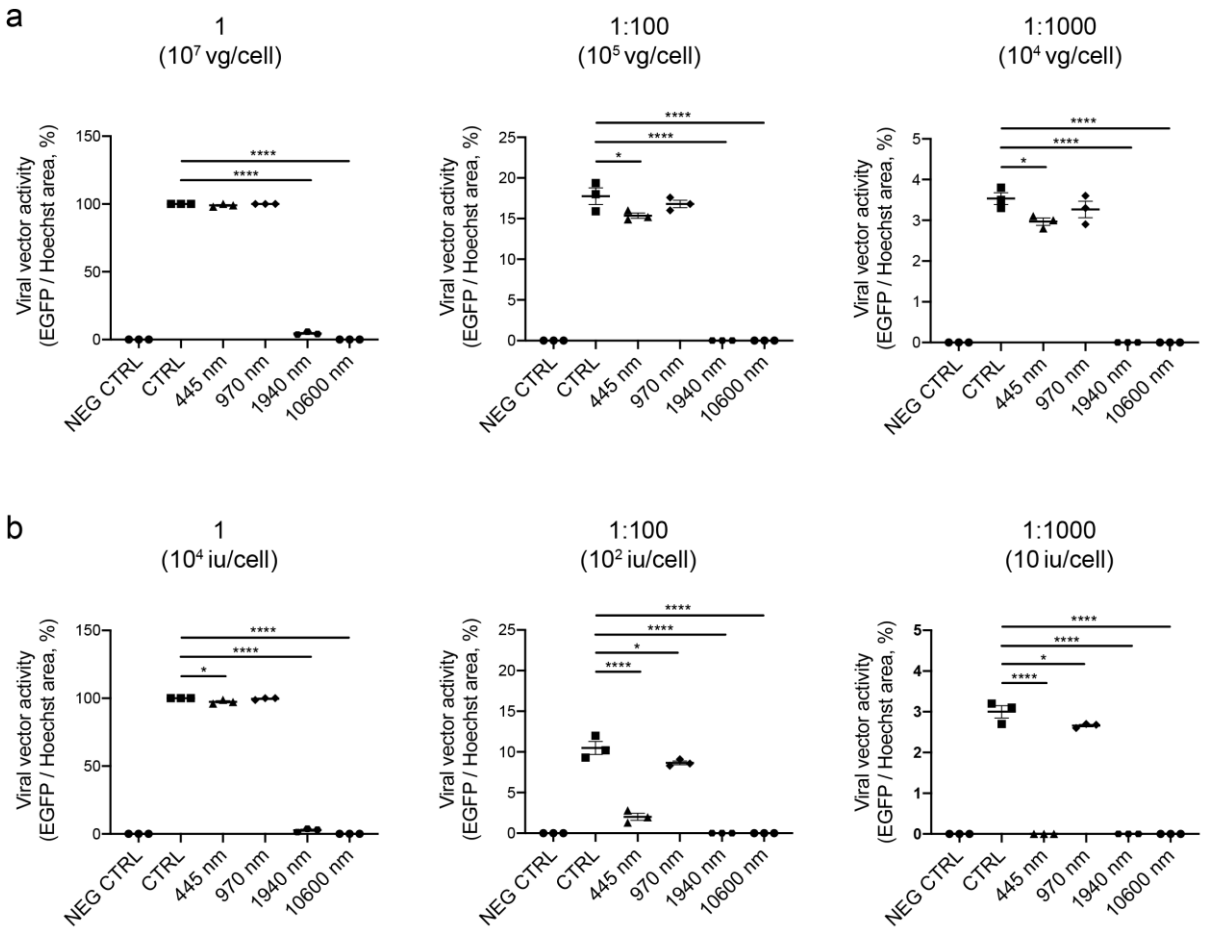

Supplementary Figure 2. Efficiency of multiple laser wavelengths in inactivating serially diluted AAV and LV vectors.

a. Quantification of viral vector activity upon transduction of HEK293 cells with a drop (1 µl) of AAV-EGFP at the indicated number of vg/cell, in control conditions (CTRL) or exposed to the indicated laser wavelengths for 2 s. * $P < 0.05$; *** $P < 0.001$; **** $P < 0.0001$. Cells not exposed to any vector represent the negative control (NEG CTRL).

b. Quantification of viral vector activity upon transduction of HEK293 cells with a drop (1 µl) of LV-EGFP at the indicated number of iu/cell, in control conditions (CTRL) or exposed to the indicated laser wavelengths for 2 s. * $P < 0.05$; *** $P < 0.001$; **** $P < 0.0001$. Cells not exposed to any vector represent the negative control (NEG CTRL).

The y-axis has a different scale in the various panels for clarity. The 1:10 dilution, corresponding to 10^6 vg/ml for AAV-EGFP and 10^3 iu/ml for LV-EGFP, are shown in Figure 1, as these represent the lowest vector dose resulting in 100% cell transduction.

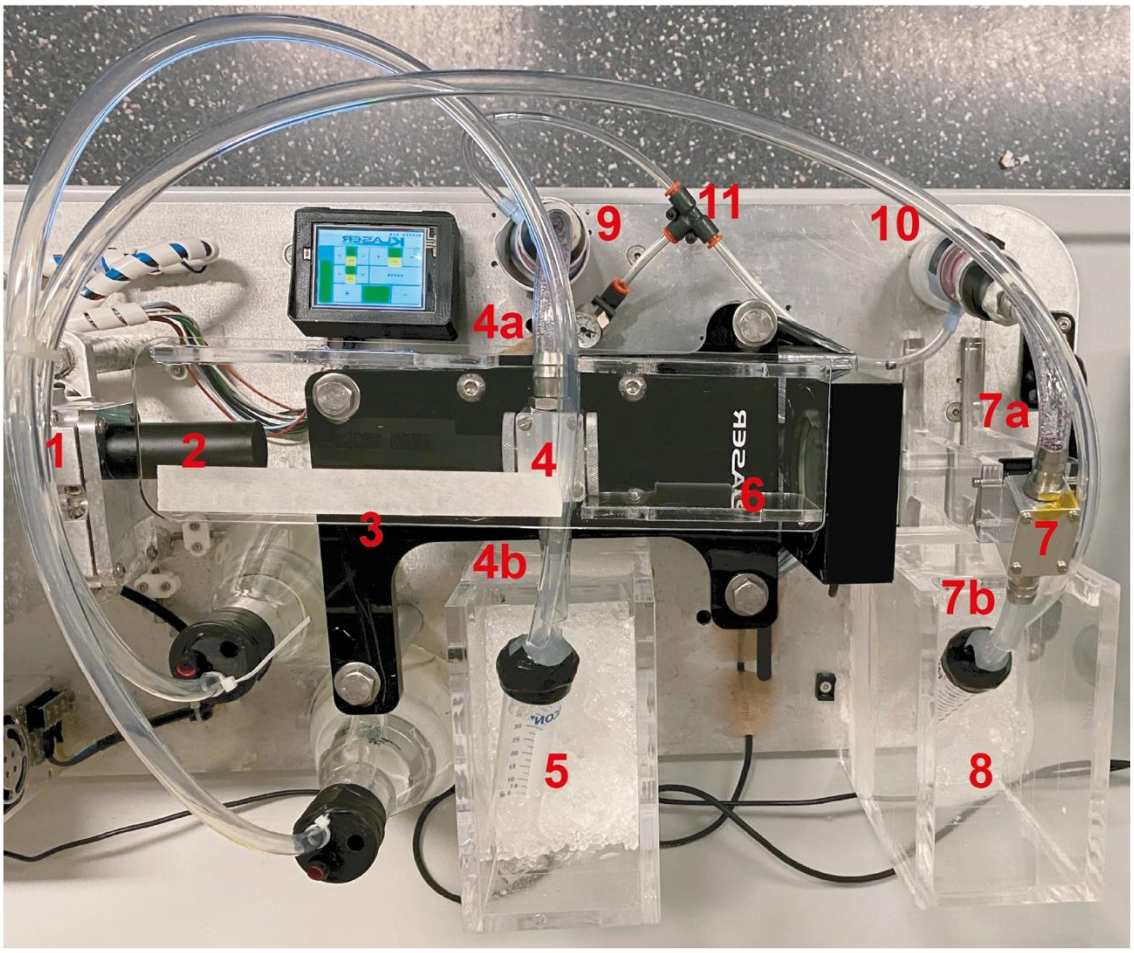

Supplementary Figure 3. Real image of our laser prototype connected with the new nebulizer.

1. Laser source; 2. Beam expander 5X; 3. Safety cover; 4. Laser chamber; 4a Aerosol inlet; 4b. Aerosol outlet; 5. Cooling tank for treated aerosol condensation; 6. Head power meter; 7. Control chamber (no laser); 7a. Control aerosol inlet; 7b Control aerosol outlet; 8. Cooling tank for control aerosol condensation; 9. Aerosol generator for laser treatment; 10. Aerosol generator for control; 11. T-junction deviator.

Supplementary Methods

Manufacturing details of a new nebulizer preserving microbial viability

The new nebulizer was generated by adapting a commercially available aerosol system relying on Venturi effect (Nebula, Air Liquid Healthcare). In particular, we used a 10 MHz DDS function generator, with digital control and arbitrary capability (Aim-TTi, #TG1010A) to control a piston air pump (Omron, #C102 Total) to operate at 3 Hz with 41% duty cycle. The pump was connected to the nebulizer by a 2 m long silicon tube. At the upper extremity of the nebulizer, the original nasal douche was replaced with a steel coupler to insert a plastic tube (internal diameter 7.5 mm) to collect and eventually condense aerosol droplets. The start push-button was eliminated, together with all inlet valves to allow air flow directly from the pump. A small hole was created in the lateral wall of the nebulization chamber to ensure the safe introduction of pathogens in the system.

Characteristics of the CO_2 laser source

The laser source used in this study is a radio frequency CO_2 laser (RF-CO_2 laser, Coherent). The peculiarities of this laser source are its high brightness, which allows the concentration of the emitted energy to reach a very high irradiance, and the generation of high-frequency variable cycle pulses (15 KHz) and variable duty cycle pulses (47%), which result in high average power output (14.1 W) from the outlet laser chamber. This brings the following advantages:

- Good beam quality immediately out of the waveguide
- Excellent stability of output power
- Short rise and fall time
- Wide range of duty cycle
- Possibility of air-cooling
- Possibility to modulate the output power
- Long lifetime
- High mechanical resistance

Integration of nebulizer and laser source in our prototype

The nebulizer described in **Figure 2c** was integrated into a prototype for laser irradiation of the generated aerosol, as schematically represented in **Figure 2f** and in the real image in **Supplementary Figure 3**. A T-junction deviator at the end of the silicon tube supplies the two aerosol generators with the same intensity and flow rate, directing it in the two chambers (laser and control). To avoid any variation of the Venturi effect and possible secondary Venturi effects, the internal diameter of the inlet tube to the chambers has the same diameter as the chambers themselves.

Similarly, the diameter of the aerosol inlet and outlet tubes from the two chambers to the cooling falcons is kept constant. In this way both pressure and flow rate remain constant, with a measured flow rate of 0.6 m/s.

A laser Power Meter apparatus with a thermophilic head of 50 mm measures the outlet laser emission (Power Meter Ophir Nova) (item 6 in **Figure 2f** and **Supplementary Figure 3**).

Both the laser chamber and control chamber (items 4 and 7 in **Figure 2f** and **Supplementary Figure 3**), consist of two parallelepipeds of identical shape and volume, 7.5 mm in length.

The aerosol spends 12.5 ms to cross either chamber, at a speed of 0.6 m/s (airflow rate is measured by a digital anemometer with a hot wire sensor, Trotec Ta300). Two zinc-selenide (ZnSe) windows, transparent to the 10600 nm wavelength allows the laser beam to penetrate the laser chamber (item 4 in **Figure 2f** and **Supplementary Figure 3**), but not in the control chamber (item 7 in **Figure 2f** and **Supplementary Figure 3**).

Close to the output of the laser source, a 5X beam expander is inserted (item 2 in **Figure 2f** and **Supplementary Figure 3**) to obtain a final laser beam area of 0.442 cm^2.

Laser parameters in our experimental settings

Peak Power: 30 W

Pulse frequency: 15 KHz

Duty cycle: 47%

Average Power: 14.1 W

Average Irradiance: 31.9 W/cm^2

Energy: 0.176 J

Supplementary Table 1. Laser parameters used for irradiation in static conditions (Figure 1c-f).

	445 nm	970 nm	1940 nm	10600 nm
Laser Power	8 W	15 W	7 W	6 W
Irradiance	40 W/cm^2	76 W/cm^2	35.7 W/cm^2	30.6 W/cm^2
Energy	16 J	30 J	14 J	12 J

Manufacturing details of a real laser device for air sterilization

The core of the device, its functioning and multiple possible realizations are described in Results and **Figure 4**. Additional details relevant for manufacturing are:

- The sterilization camera is 50 cm long, 7 cm in diameter, made of aluminum and internally coated with Teflon.
- The laser beam is centered on the mirror hole thanks to an alignment system composed by a couple of horizontal and vertical translators.
- The CO_2 laser is constantly cooled by the air exiting from the sterilization camera by convection.
- The progressive increase in size of the laser beam during its bouncing back and forth between mirrors depends on the propagation distance (z) following the Gaussian beam theory and according to the following formula:

$$w(z) = w_0 \sqrt{1 + \left(\frac{z}{z_R}\right)^2}$$

Where

$$z_R = \frac{\pi w_0^2}{\lambda}$$

is the so-called Rayleigh range, with w_0 the spot size at the laser output (beam waist) and λ the laser wavelength.